Single Photon Fluorescent Microlithography for Live-Cell Imaging

DARÍO KUNIK,[1,2]* PEDRO F. ARAMENDIA,[1,3] AND OSCAR E. MARTÍNEZ[1,2]
[1]*Dpto. de Física. Fac. de Ciencias Exactas y Naturales, Universidad de Buenos Aires, C1428EHA, Buenos Aires, Argentina*
[2]*CONICET Consejo Nacional de Investigaciones Científicas y Técnicas, Argentina*
[3]*INQUIMAE and Departamento de Química Inorgánica, Analítica y Química Física. Fac. de Ciencias Exactas y Naturales, Universidad de Buenos Aires, C1428EHA, Buenos Aires, Argentina*

KEY WORDS microscopy; lithography; microfluidics; colocalization; photopolymerization

ABSTRACT Using fluorescent dyes to trigger the polymerization of a commercial polyurethane resin allows a rapid fabrication of micrometer and submicrometer sized fluorescent structures by one-photon absorption. Here, we show that standard He–Ne lasers emitting at 632.8 nm can be used to start the photopolymerization and that very low laser power is required. This procedure allows the fabrication of fiduciary fluorescent references on standard glass coverslips, mica sheets, or gold-coated coverslips for laser scanning or standard fluorescent microscopy. The biocompatibility of the polymerized resin with cells in culture was tested by growing *Xenopus* melanophores and a standard laser scanning microscope was used to demonstrate that it is possible to use equipment readily available in several laboratories. We show that fluorescent structure with less than 10 nm in height may be used as references in fluorescence microscopy allowing a smooth environment for cell growth. Different dyes were tested and the conditions for one-photon polymerization were outlined. *Microsc. Res. Tech. 73:20–26, 2010.*

INTRODUCTION

The use of fluorescent tags and markers in microscopy is a well-established technique in many fields including cell biology and microfluidics. In many of these applications because of their extension in time, the drift of the sample (mostly of thermal origin) or even cell movements limit the precision of spatial correlation of information gathered at different times (Carter et al., 2007). Particularly, stringent conditions are required for nanometer size localization or colocalization (Koyama-Honda, 2005), tracking (Levi et al., 2005), and imaging beyond the diffraction barrier (Axelrod, 2001; Betzig and Trautman, 1992; Betzig et al., 2006; Gustafsson, 2000; Hofmann et al., 2005; Willig et al., 2006).

A way to overcome this problem has been recently published (Costantino et al., 2005) by using a lithographic technique to fabricate fluorescent reference grids. The technique is based on mixing a UV-curing polymer with the desired fluorescent dye and curing the resin with an ultrashort infrared laser pulse, thus avoiding the bleaching of the dye by using UV-curing light. This technique was proved to be useful to fabricate several types of micrometer sized structures, including fluorescent reference marks and poly dimethylsiloxane (PDMS) stamp molds for microcontact printing and microfluidics. In that article, it was also shown that the fluorescent patterned microstructures are biocompatible with cultures of mammalian cell lines and hippocampal neurons. More recently, it was shown that because of substrate surface effects tens of nanometers high-fluorescent structures could be fabricated, despite the much larger length of the focal volume of the excitation beam (Kunik et al., 2007). The technique allowed rapid prototyping as a very simple program and can scan the sample while the laser is turned on and off. The disadvantage of this two-photon technique is the requirement of a relatively high-power ultrafast laser not so readily available at every confocal microscope facility.

In this work, we present an alternative technique that allows the fabrication of fluorescent structures in the micrometer and submicrometer ranges by using low-power single photon excitation. The technique relies in the use of fluorescent dyes that trigger the photopolymerization of the resin. Very low laser power, in the range of microwatts, is necessary, thus making the technique readily available in any scanning microscope set up. The polymer used in this work is the same as reported before (Costantino et al., 2005). Hence, all the applications previously reported such as reference grids, molds for stamping, or construction of microfluidic channels are possible with this technique. In this work, we also show that the conditions required to build the different structures, the possibility of using different dyes, and the biocompatibility of the structures by growing cells over a grid. Structures can be made of 10–20 nm and are still visible in the fluorescent or confocal microscope, providing a very smooth environment for cell growth. We also demonstrate that

*Correspondence to: Darío Kunik, Dpto. de Física. Fac. de Ciencias Exactas y Naturales, Universidad de Buenos Aires, C1428EHA, Buenos Aires, Argentina. E-mail: dkunik@df.uba.ar

Received 15 May 2009; accepted in revised form 16 May 2009
DOI 10.1002/jemt.20748
Published online 12 June 2009 in Wiley InterScience (www.interscience.wiley.com).

it is possible to fabricate the samples using a standard commercial confocal microscope.

MATERIALS AND METHODS

Experimental Set Up and Nanolithography Procedure

The experimental set up is basically analogous to the one reported previously (Costantino et al., 2005; Kunik et al., 2007), but in this work, we use continuous wave (CW) lasers to start the photopolymerization by one-photon absorption. The polymerization chain is initiated not only by the additives of the adhesive photocurable mixture used but also by the selected dye molecule added to the commercial mixture. The choice of the laser to excite the dye to trigger the polymerization process depends on the absorption spectrum of the dye used. We used cyanine (ADS675MT, American Dye Source, Quebec, Canada) and oxazine dyes (Nile-Blue 690 Perchlorate, Exciton, OH) excited with a He–Ne laser emitting at 632.8 nm, and we tested different infrared cyanines dyes (ADS740, ADS760, and ADS775PI, American Dye Source, Quebec, Canada and HITC Iodide and LDS821, Exciton, OH) excited with a Ti:Sapphire laser in CW mode tuned to match the absorption spectrum of these dyes. The technique is illustrated in Figure 1 where a scheme of the set up is presented. A cw laser is focused onto the sample by means of a high numerical aperture air objective (UplanSapo 40x, NA = 0.9, Olympus, Tokyo, Japan) placed in an inverted microscope configuration. A blend of the UV-cure adhesive (NOA 60, NOA 63 or NOA65, Norland Products Cranbury, NJ) with a highly concentrated solution of fluorescent dye in methanol or acetone is prepared, as explained later. A drop of this blend is placed on top of a standard glass cover slip, of a mica sheet, or of a gold coated cover slip to begin the photopolymerization process. The power of the laser is adjusted by inserting neutral density filters in the beam path. A shutter is interposed in the beam way to control the pattern design. The sample holder is motorized in the three axes by means of xyz stages (Newport 461 Series Newport Irvine, USA) and closed-loop actuators with a travel range of 12.5 mm of travel with a speed range between 1 and 400 μm s^{-1} (z612b Thorlabs, Newton, NJ). The smallest step accessible for the motors was 50 nm. The control of the focus was made by means of a CCD camera imaging the back reflection of the laser beam, and the sample focus was adjusted to minimize the image size in the CCD camera. A kinematic mirror mount used as a platform allowed the tilt correction of the cover slip plane relative to the translation stage axes to avoid focus walk off during the sample scan. As the beam was focused down to less than a micrometer in diameter, the focal depth resulted in a few micrometers, thus rendering this focus control essential for a homogeneous treatment along the scan. A 1-μm control over a scan of 1 mm requires setting the sample within 1 m rad of the scanning axis. The size of

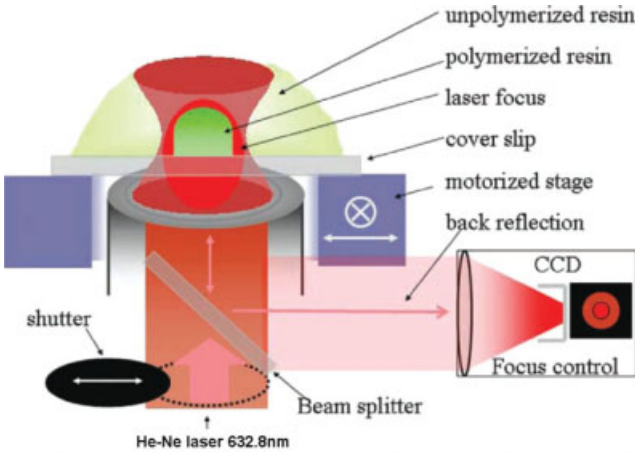

Fig. 1. Schematic of the set up. [Color figure can be viewed in the online issue, which is available at www.interscience.wiley.com.]

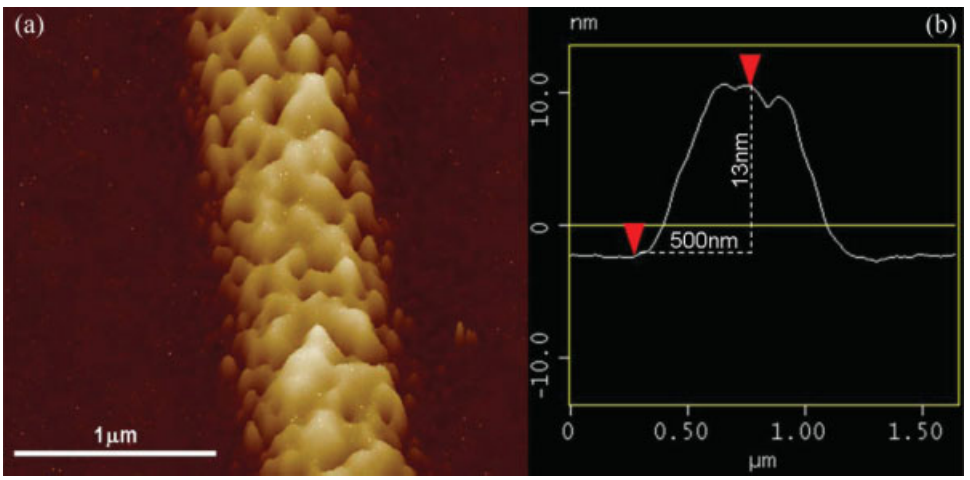

Fig. 2. Nanostructure fabricated by one-photon absorption polymerization. (**a**) 3D Reconstruction of a topographic AFM image in tapping mode. (**b**) Average crosssection. The line has ~13 nm in high and less than 1 μm in wide The He–Ne laser power was 35 μW, the scanning speed was 16 μm/s, and the blend was NOA60-ADS675MT (1 mM). [Color figure can be viewed in the online issue, which is available at www.interscience.wiley.com.]

the focused beam was measured by detecting the scattered light on a gold nanoparticle 80 nm in diameter, resulting in a FWHM of 800 nm.

As the sample is scanned, the polymerization reaction takes place in the illuminated region. The polymerization grade depends on both laser power and the time it takes to the beam to scan a given point and on the dye concentration.

Alternatively, we used a standard commercial confocal microscope (FV1000, Olympus Tokyo Japan) to drive the photopolymerizable blend by scanning the beam instead of the sample. Similar results were obtained in both cases. The same microscope was used to take fluorescence and transmission images. To measure the height of the polymer lines and their detailed structure with nanometer resolution, an atomic force microscope (AFM, Veeco-Digital Instruments Nano-Scpope IIIa-Quadrex, Woodbury, NJ) was used in tapping mode.

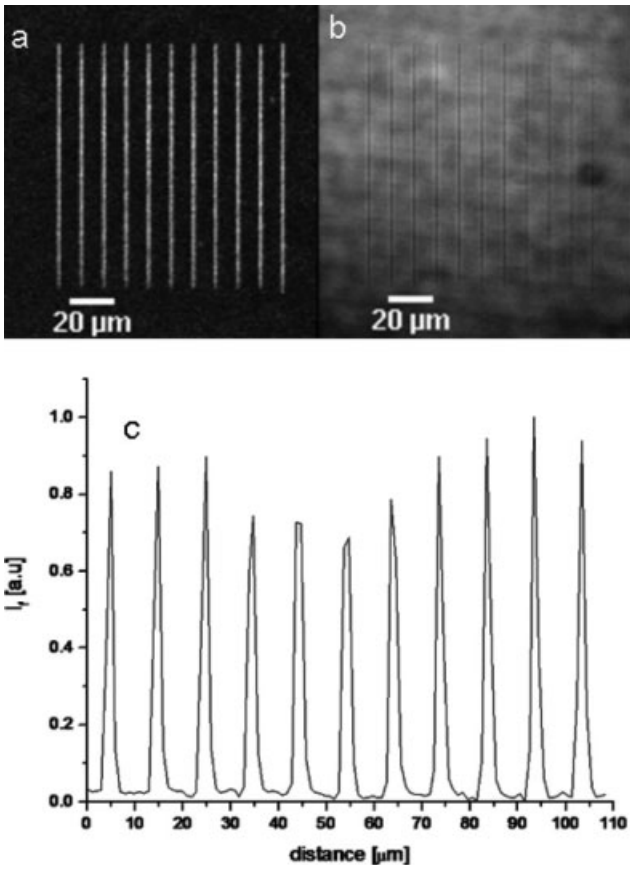

Fig. 3. Fluorescent and transmission images of the nanostructure. (**a**) Confocal fluorescent image of 10-µm separated lines, (**b**) transmission images, and (**c**) average crosssections of the lines shown in (a). The He–Ne laser power was 35 µW, the scanning speed was 16 µm/s, and the blend was NOA60-ADS675MT (1 mM).

Blend Preparation

Different polymer–dye blends were prepared changing both the UV-curing adhesive and the dyes used. The following steps were followed: (1) select an adequate cosolvent for both the dye and the adhesive, in most cases ethanol, methanol, and acetone worked well, we used methanol for our reported essays. (2) Make a concentrated solution of the dye in the solvent, typically 10 mM in methanol. (3) Add the dye solution to the polymer resin to a final concentration of 1 mM. (4) Place a coverslip on the microscope and set the focus at the surface. (5) Place a drop of blend on the coverslip. (6) Scan the laser to draw the desired structure. (7) Rinse the coverslip immersing it in ethanol and acetones. A final rinse of few seconds in methylene chloride is helpful to efficient remove remanent unpolymerized resin.

Cell Culture

Immortalized *Xenopus laevis* melanophores permanently transfected with enhanced green fluorescent protein (EGFP)-tagged XTP (Levi et al., 2006), a *Xenopus* homolog of tau protein (Olesen et al., 2002), were cultured as described by (Rogers et al., 1997). The number of melanosomes in the cell was reduced by treatment with phenylthiourea (Gross et al., 2002). For microscopy measurements, the cells were grown for 2 days on petri dishes. To include the coverslip with the fluorescent grid, a hole was performed on the petri dishes, and the coverslip was glued with a standard

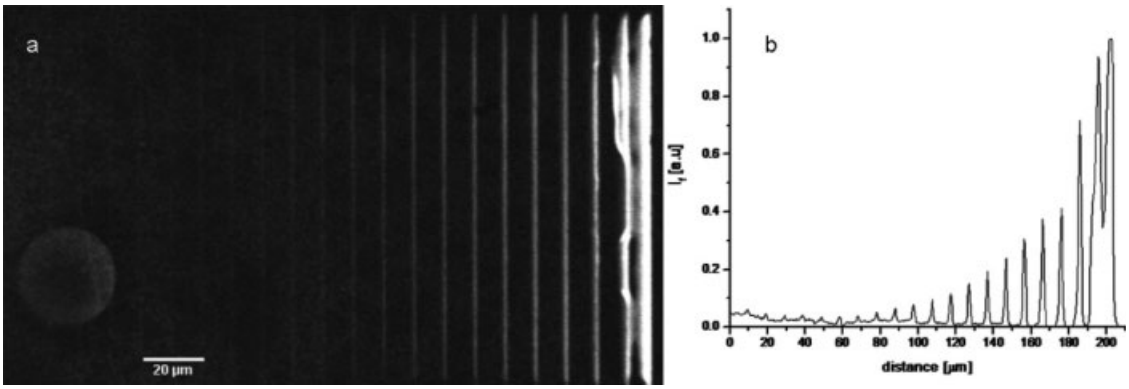

Fig. 4. Different lines scanning the speed from 6 to 46 µm/seg. (**a**) Confocal fluorescent images of the lines and (**b**) average crosssection.

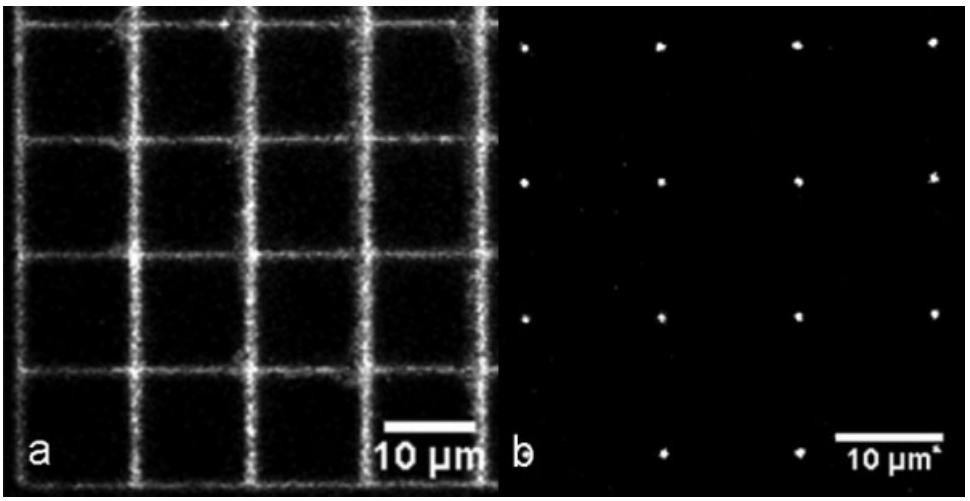

Fig. 5. Fluorescent grid made using a standard confocal microscope. (**a**) Fluorescent grid of 12 μm side. Each line was scanned 30 times, the laser power was 170 μW, the speed was 200 μs/px, and pixel size was 600 nm. (**b**) Arrangement of fluorescent dots. The power of the laser was 5 μW, the exposition time was 0.5 s, and in both case, the blend used was NOA60-ADS675MT (1 mM), and the laser wavelength was 635 nm.

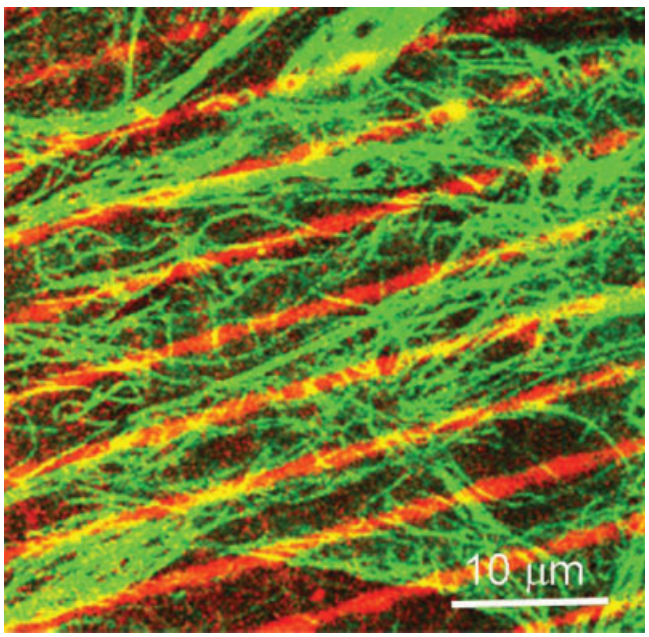

Fig. 6. Two-color LSM images of cells on red fluorescent grids, using ADS675MT as dye. *Xenopus laevis* melanophores permanently transfected with enhanced green fluorescent protein (EGFP)-tagged XTP. [Color figure can be viewed in the online issue, which is available at www.interscience.wiley.com.]

commercial epoxi. All measurements were performed at room temperature.

RESULTS

Fiduciary Marks and Focal References for Fluorescent and Confocal Microscopy

In Figure 2, an atomic force microscope image of a line prepared with a blend of NOA60 adhesive and 1 mM ADSS675MT (prepared in methanol) is presented. A He–Ne laser at 632.8 nm was used with a power in the sample of 35 μW, and the line was drawn scanning the sample at a speed of 16 μm/s. Under this illumination conditions, a very shallow structure is obtained with an average height of 13 nm. The width is diffraction limited to almost 1 μm at the line base. The fact that the lines are much thinner than the 2.5 μm focus depth of the beam is due to the adsorption of the dye molecules at the glass surface thus favoring the polymerization process near the surface. The same lines are shown in Figure 3 as appear in a confocal microscope. The lines are clearly visible both in transmission and fluorescent modes. The images were taken with a FV 1000 Olympus microscope using the 635 nm laser line and to acquire the fluorescent signal of the sample the spectral modulus was used collecting light between 690 and 710 nm.

The height and, hence, the brightness of the lines when observed in the fluorescent mode of the confocal microscope grows monotonically with the exposition time (inverse of the scan speed) as observed in Figure 4 where different lines were drawn scanning at speeds ranging from 6 to 46 μm/s at constant beam power. This corresponds to an eightfold increase in the dose from one end to the other. The increase in the brightness is not linear because both the height and the width are changing in a nonlinear manner. The lines drawn at slower scans show an important lateral broadening due to the nonlinearity established by the existence of a threshold for the onset of the polymerization. As the threshold is exceeded at the edges of the beam profile, the line broadens significantly. This effect does not appear when the two-photon triggering method is used, thus allowing in the former case the design of taller structures (above 1 μm) without significant broadening.

From the exposition time, i.e., the ratio between the beam size and the scan speed, the beam intensity and

the dye absorption crosssection, it can be inferred that the polymerization process is very inefficient, and more than 100 thousand photons must be absorbed by each molecule before the process occurs significantly. This inefficient process is the clue to having a strong remanent fluorescence as most of the dye molecules will not have undergone a reaction initiation. The number is also adequate to prevent bleaching of the dye before the process takes place.

Similar lines were obtained using adhesives of different viscosities (NOA 60, NOA 63, or NOA65, Norland Products Cranbury, NJ), ranging from 300 to 2500 cps. The photoinitiation process was observed with cyanine dyes such as ADS740PP, ADS760MP, and ADS775PI, American Dye Source, Quebec, Canada and HITC Iodide and LDS821, Exciton, OH. In all the cases, the pump laser was a CW Ti:sapphire tuned to an adequate wavelength for each dye. The oxazine dye Nile-Blue 690 Perchlorate, Exction, OH, was also successfully used as photoinitiator excited with a He–Ne laser at 633 nm. To ensure that the UV photosensitizer played no role in the process, a special batch of NOA60 resin without the UV sensitive additive was provided by the manufacturer (Norland Products) that yielded similar results

The feasibility of using a commercial standard microscope to fabricate fluorescent structures was also tested. As is shown in Figure 5a, a grid of 12 μm side was obtained by scanning the beam. Each line was scanned 30 times. The power of the 635 nm laser was 170 μW, the scanning speed was 200 μs/px, and the pixel size was 600 nm. In Figure 5b, we show an

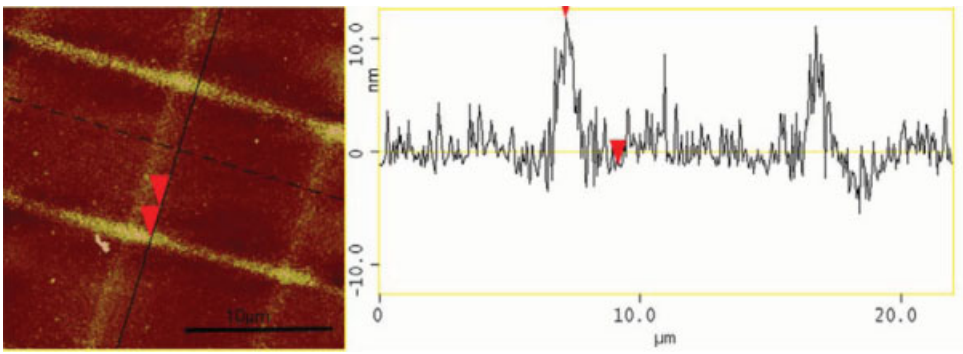

Fig. 7. Topographic AFM image of the grid used to grow the cells. The height of the lines are smaller than 10 nm, and the wide is 1 μm on the basis of the line. [Color figure can be viewed in the online issue, which is available at www.interscience.wiley.com.]

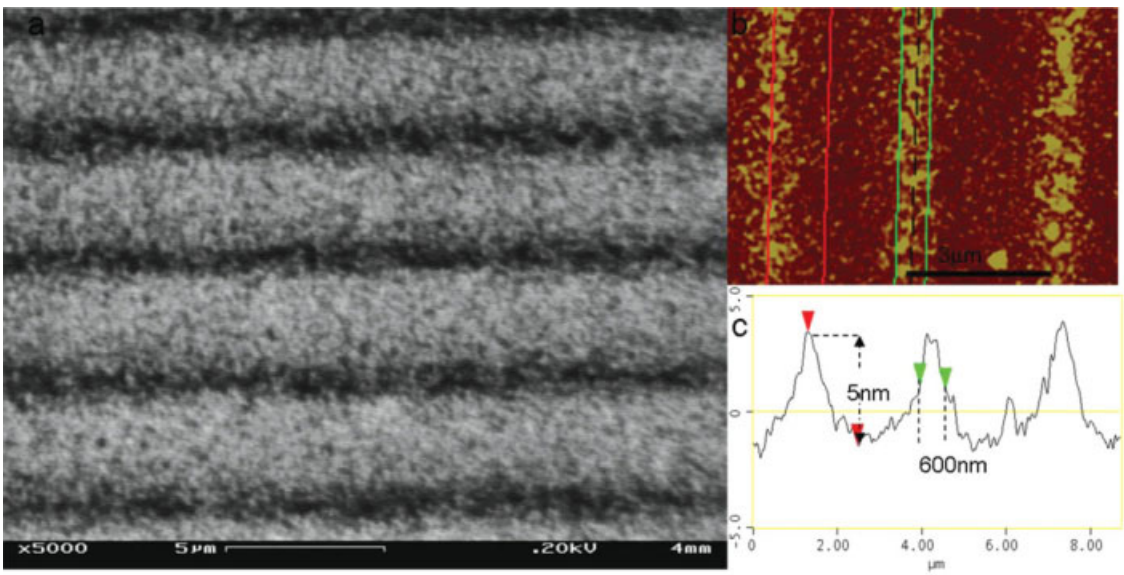

Fig. 8. Diffraction grid done on a gold-coated cover slip. The separation between lines is 3 μm. The blend used was NOA60-ADS675MT (1 mM). The He–Ne laser power was 250 μW, and the scanning speed was 100 μm s^{-1}. [Color figure can be viewed in the online issue, which is available at www.interscience.wiley.com.]

arrangement of dots obtained by focusing the beam in different points and keep it by 0.5 s. The wavelength of the laser was 635 nm, and the power was 5 μW. The blend used was NOA60-ADS675MT, and the concentration of the dye was 1 mM. The total time needed to fabricate the grid of 120 by 120 μm was of the order of 15 min, whereas for the dots, only a few minutes were necessary.

The biocompatibility of the grids was tested growing EGFP transfected *Xenopus laevis* cells as shown in Figure 6. The grid lines were only 10-nm high as shown in the atomic force microscope image in tapping mode shown in Figure 7. The crosssection indicates the extremely small height of the lines, despite of what they are still clear in the confocal fluorescent image shown in Figure 6.

Another application for which the system was tested was growing a diffraction grating on top of a thin (10 nm) gold film over a glass substrate. In this case, the NOA60-ADS675MT blend was used, and the illumination was done through the gold film The gold film transmission was near to 50%, the incident power after the objective was close to 250 μW, and the scanning speed was 100 μm s^{-1}. The structures prepared were observed by means of a field emission scanning electron microscope as shown in Figure 8. The atomic force microscope show that the lines prepared had a height of 5 nm and a diffraction limited width of 600 nm. Surprisingly, despite the expected quenching of the fluorescence due to the gold proximity (Novotny, 2006), the polymerization process developed. We assume this is due to the existence of many regions of increased intensity (hot spots) originated by the rough structure of the gold film. These hot spots compensated the increased decay rate due to quenching yielding a similar structure at slightly higher powers. This dielectric structure build on top of metal films proved useful for plasmonic device fabrication.

Up to the moment, we cannot provide a mechanistic explanation of the polymerization process, but we can give some hints on the nature of the photoinitiation steps. Cyanine dyes have been used to initiate photopolymerization using visible light (Kabatc et al., 2005, 2006; Chatterjee et al., 1988). The initiation of the chain reaction is due to an intramolecular electron transfer reaction in the cyanine-counter ion pair. In the present experiments, the polymerization is initiated by cyanine dyes having very different chemical structures. One can expect HITC iodide to initiate polymerization by photoreduction of the cyanine cation by iodide, but this will certainly not be the case in the tosilate salt or the anionic cyanine dye with sodium counterion. Moreover, although cyanines are all efficient photoinitiators, oxazine dyes, such as Nile Blue are effective (but photobleach to a great extent), whereas Methylene Blue is inactive and completely photobleaches in the polymerization mixture.

In view of all the previous discussion, at this point we can only speculate that the photopolymerization initiation event is a low-efficiency reaction of an excited state of the cyanine (presumably a singlet, considering the very low triplet quantum yield of cyanine dyes) with one component of the curing mixture.

CONCLUSIONS

We have shown that fluorescent patterns can be easily obtained on standard coverslip with readily available equipment in standard microscopy laboratories. When compared with the previous work, single-photon processing allows the use of very low-power CW lasers in the range of 1 mW or less. The structures obtained are diffraction limited in the lateral dimensions but can be made as small as 5 nm in height and still be observable in the fluorescence microscope.

Several different adhesives were tested with very distinct viscosities ranging from 300 to 2,500 cps. Oxazine and cyanine dyes proved adequate for the initiation mechanism as long as the laser wavelength is appropriately tuned.

The power and exposition times indicate that the dye molecules undergo at least 10^5 fluorescent transitions per polymerization reaction, indicating that the mechanism is very inefficient, allowing an adequate control of the process without an avalanche growth. This inefficiency is also essential for the large number of remanent virgin molecules left in the polymer for fluorescent imaging. The inefficiency is not so large as to give rise to bleaching of the molecule before the reaction takes place.

The mechanism also worked on top of very thin gold films excited by transmission, permitting the construction of plasmonic devices and lithography on gold.

ACKNOWLEDGMENTS

The authors thank V. Levi (Universidad de Buenos Aires, Buenos Aires Argentina) for supplying transfected *Xenopus* cells.

REFERENCES

Axelrod D. 2001. Total internal reflection fluorescence microscopy in cell biology. Traffic 2:764–774.

Betzig E, Trautman JK. 1992. Near-field optics—Microscopy. Spectroscopy, and surface modification beyond the diffraction limit. Science 257:189–195.

Betzig E, Patterson GH, Sougrat R, Lindwasser OW, Olenych S, Bonifacino JS, Davidson MW, Lippincott-Schwartz J, Hess HF. 2006. Imaging intracellular fluorescent proteins at nanometer resolution. Science 313:1642–1645.

Carter AR, King GM, Perkins TT. 2007. Back-scattered detection provides atomic-scale localization precision, stability, and registration in 3D. Opt Express 15:13434–13445.

Chatterjee S, Gottschalk P, Davis PD, Schuster GB. 1988. Electron-transfer reactions in cyanine borate ion pairs: photopolymerization initiators sensitive to visible light. J Am Chem Soc 110:2326–2328.

Costantino S, Heinze KG, Martinez OE, De Koninck P, Wiseman PW. 2005. Two-photon fluorescent microlithography for live-cell imaging. Microsc Res Tech 68:272–276.

Gross SP, Tuma MC, Deacon SW, Serpinskaya AS, Reilein AR, Gelfand VI. 2002. Interactions and regulation of molecular motors in *Xenopus melanophores*. J Cell Biol 156:855–865.

Gustafsson MGL. 2000. Surpassing the lateral resolution limit by a factor of two using structured illumination microscopy. J. Microsc (Oxford) 198:82–87.

Hofmann M, Eggeling C, Jakobs S, Hell SW. 2005. Breaking the diffraction barrier in fluorescence microscopy at low light intensities by using reversibly photoswitchable proteins. Proc Natl Acad Sci USA 102:17565–17569.

Kabatc J, Jędrzejewska B, Pączkowski J. 2005. Electron transfer processes in photoinitiating systems composed of hemicyanine *sec*-butyltriphenylborate ion pairs. Polym Bull 54:409–416.

Kabatc J, Jędrzejewska B, Pączkowski J. 2006. Asymmetric cyanine dyes as fluorescence probes and visible-light photoinitators

of free radical polymerization processes. J Appl Polym Sci 99: 207–217.

Koyama-Honda I, Ritchie K, Fujiwara T, Iino R, Mirakoshi H, Kasai RS, Kusumi A. 2005. Fluorescent imaging for monitoring the colocalization of two single molecules in living cells. Biophys J 88:2126: 2136.

Kunik D, Ludueña SJ, Costantino S, Martínez OE. 2007. Fluorescent two-photon Nanolithography. J Microsc (Oxford) 229:540–544.

Levi V, Ruan QQ, Graton E. 2005. 3-D particle tracking in a two-photon microscope: application to the study of molecular dynamics in cells. Biophys J 88:2919–2928.

Levi V, Serpinskaya AS, Gratton E, Gelfand V. 2006. Organelle transport along microtubules in *Xenopus melanophores*: Evidence for cooperation between multiple motors. Biophys J 90:318–327.

Novotny L, Hetch B. 2006. Principle of nano-optics. New York: Cambridge University Press.

Olesen OF, Kawabata-Fukui H, Yoshizato K, Noro N. 2002. Molecular cloning of XTP, a tau-like microtubule-associated protein from *Xenopus laevis* tadpoles. Gene 283:299–309.

Rogers SL, Tint IS, Fanapour PC, Gelfand VI. 1997. Regulated bidirectional motility of melanophore pigment granules along microtubules in vitro. Proc Natl Acad Sci USA 94:3720–3725.

Willig KI, Rizzoli SO, Westphal V, Jahn R, Hell SW. 2006. STED microscopy reveals that synaptotagmin remains clustered after synaptic vesicle exocytosis. Nature 440:935–939.